




Cite this: *Environ. Sci.: Nano*, 2017, 4, 2186

# Quantitative evaluation and *in vivo* visualization of mercury ion bioaccumulation in rotifers by novel aggregation-induced emission fluorogen nanoparticles†

Yusheng Jiang,<sup>‡abc</sup> Tao He,<sup>‡bd</sup> Yuncong Chen,<sup>e</sup> Yinlan Ruan,<sup>f</sup> Yabin Zhou,<sup>c</sup> Ben Zhong Tang,<sup>\*e</sup> Jianguang Qin<sup>\*b</sup> and Youhong Tang <sup>\*c</sup>

In this study, a specifically-designed aggregation-induced emission fluorogen (AIEgen) with nanoparticle aggregates was used to quantitatively evaluate the bioaccumulation of Hg<sup>2+</sup> and visualize Hg<sup>2+</sup> kinetics *in vivo* within the rotifer *Brachionus plicatilis* for the first time. Quantitative results showed that a sharp drop in Hg<sup>2+</sup> concentration occurred at the very beginning in the medium containing rotifers and Hg<sup>2+</sup>, showing a quick initial uptake of Hg<sup>2+</sup> by the rotifers, and then the concentration in the medium plateaued after 5 min. With an increase in rotifer density, the amount of bioaccumulation increased in the rotifer. However, the bioaccumulation efficiency of Hg<sup>2+</sup> decreased from 5.28 µg mg<sup>-1</sup> h<sup>-1</sup> at a low rotifer density of 0.093 mg mL<sup>-1</sup> to 2.61 µg mg<sup>-1</sup> h<sup>-1</sup> at a high rotifer density of 0.375 mg mL<sup>-1</sup>. Moreover, the fluorescence images and spectra results illustrate that the ingestion of Hg<sup>2+</sup> by the rotifer was *via* its mouth surrounded by the ciliary corona to the digestive tract, and Hg<sup>2+</sup> could not permeate into the body integument through diffusion during the study period. Hg<sup>2+</sup>-induced fluorescence in rotifers dissipated in 6 h after staining, possibly through defecation and excretion. This study indicates that inorganic mercury can be quickly ingested by a rotifer *via* feeding, but is unlikely deposited as methylated mercury in rotifer tissues.

Received 3rd July 2017,  
Accepted 12th September 2017

DOI: 10.1039/c7en00599g

rsc.li/es-nano

## Environmental significance

The bioaccumulation of Hg<sup>2+</sup> in aquatic organisms is astonishing. However, traditional methods are unable to quantify mercury dynamics inside small aquatic invertebrates because these methods only provide a “snapshot” of organisms for a particular time and life stage. In this study, a specifically-designed aggregation-induced emission fluorogen with nanoparticle aggregates was used to quantitatively evaluate the bioaccumulation of Hg<sup>2+</sup> and visualize Hg<sup>2+</sup> kinetics *in vivo* within a rotifer for the first time. The results illustrated that Hg<sup>2+</sup> could not permeate into the body integument through diffusion, and Hg<sup>2+</sup>-induced fluorescence in rotifers dissipated after staining, possibly through defecation and excretion during the study period. This study indicates that inorganic mercury can be quickly ingested by a rotifer *via* feeding, but is unlikely deposited as methylated mercury in rotifer tissues.

## Introduction

Bioaccumulation is the process of gradual build-up of a chemical in a living organism within a trophic level, through which the concentration of the chemical in the organism exceeds that in the medium.<sup>1</sup> Some aquatic organisms are able to accumulate, retain and transform toxic chemicals within the body through biochemical and physiological processes especially in a habitat where pollutants prevail due to human activity.<sup>2</sup> Toxic substance accumulation can reduce growth and reproductive fitness, and cause genetic mutation and even death of aquatic organisms.<sup>2</sup> Therefore, toxic chemicals in algae can be transferred along the food chains to zooplankton, fish, sea mammals, and humans.<sup>3</sup>

Zooplankton is an important trophic link between primary producers and predators in an aquatic system. Rotifers are

<sup>a</sup> College of Aquaculture and Life Sciences, Dalian Ocean University, Liaoning 116023, China

<sup>b</sup> College of Science and Engineering, Flinders University, South Australia 5042, Australia. E-mail: jian.qin@flinders.edu.au; Tel: +61 8 82013045

<sup>c</sup> Centre for NanoScale Science and Technology, Flinders University, South Australia 5042, Australia. E-mail: youhong.tang@flinders.edu.au; Tel: +61 8 82012138

<sup>d</sup> College of Animal Science and Technology, Southwest University, Chongqing 400716, China

<sup>e</sup> Department of Chemistry, The Hong Kong University of Science and Technology, Hong Kong, China. E-mail: tangbenz@ust.hk; Tel: +852 2358 7375

<sup>f</sup> Institute for Photonics and Advanced Sensing, School of Physical Sciences, University of Adelaide, South Australia, 5005, Australia

† Electronic supplementary information (ESI) available. See DOI: 10.1039/c7en00599g

‡ These authors contributed equally.



widely-distributed small invertebrates in water, mainly consuming microalgae and organic detritus, and serve as food for fish, shrimp and crab.<sup>4</sup> In nature, rotifers are first level consumers that can accumulate toxic substances by grazing algae at the base of a food chain.<sup>5</sup> Rotifers are also important live food for the culture of many aquatic animals in aquaculture farms. In the laboratory, rotifers have been used as a model organism in aquatic toxicological research due to their short reproduction cycle, fast population growth and ease of culture.<sup>4</sup>

Among all the toxic substances accumulated in aquatic organisms, mercury (Hg) is one of the most dangerous and ubiquitous heavy metal pollutants in water, and is ranked the third after arsenic and lead in the list of hazardous substances.<sup>6</sup> A major concern with Hg contamination is its transfer and biomagnification in aquatic food chains. Mercury exists in many compounds, bonding with other elements such as chlorine, carbon and oxygen, and all these mercury compounds are toxic.<sup>6</sup> The mercury ion ( $\text{Hg}^{2+}$ ) can easily pass through the skin and respiratory and gastrointestinal tissues into the human body, causing damage to the central nervous system and endocrine system.<sup>7</sup> Moreover,  $\text{Hg}^{2+}$  can be converted to methyl mercury (MeHg) by a variety of microorganisms in water to interfere with the normal development of the fetal brain in humans.<sup>8</sup>

The bioaccumulation of  $\text{Hg}^{2+}$  in aquatic organisms is astonishing. However, traditional methods are unable to quantify mercury dynamics inside small aquatic invertebrates because these methods only provide a “snapshot” of organisms for a particular time and life stage, and the transfer mechanism of toxic substances along the food chain is largely unknown, especially in small aquatic organisms.<sup>9</sup> Moreover, traditional methods are limited for use in well-established laboratories, due to the requirements of sophisticated instrumentation and labor-intensive processes for sample preparation.<sup>10</sup> Therefore, there is a compelling need to develop a new methodology to detect and quantify toxic substances in aquatic organisms *in vivo* to understand the mechanisms of enrichment and transfer of  $\text{Hg}^{2+}$ .

Many previous studies have tested  $\text{Hg}^{2+}$  transformation in aquatic biota (phytoplankton, zooplankton, and fish) and analyzed the respective  $\text{Hg}^{2+}$  concentrations.<sup>11</sup> However, these studies did not provide information regarding the uptake and removal kinetics of  $\text{Hg}^{2+}$ , which are important parameters for interpreting and predicting the food-chain transfer of  $\text{Hg}^{2+}$ . It remains essentially unknown whether the accumulated  $\text{Hg}^{2+}$  in zooplankton originates from medium absorption, ingestion from food, or parental transfer. Empirical evidence exists for the dominance of food for MeHg exposure in fish, but no information is available with regard to zooplankton species.<sup>12</sup>

Aggregation-induced emission (AIE) refers to a photo-physical effect whereby light emission of a fluorogen is activated by aggregate formation to nanoparticles, which may be used as a sensing method in biological applications.<sup>13</sup> Fluorogens with AIE effects are known as AIEgens that lumi-

nesce more efficiently in the practically useful aggregate state (for example, forming nanoparticles) than in the solution state.<sup>14</sup> In an AIE system, the aggregates shine brighter than their individual parts, following the general collective quantity-effect rule. The AIE effect permits the use of highly concentrated solutions of fluorogens and their aggregates in aqueous media for sensing and imaging applications, leading to the development of fluorescence turn-on or light-up nanoprobe with a wide molecular diversity, ready structural tenability, and good biological compatibility.<sup>15</sup> The discovery of AIE has made it possible to track trace substances in small organisms through fluorescence quantification and visualization.<sup>16–18</sup>

AIEgen fluorescent probes have been developed<sup>19,20</sup> using a novel methodology based on an AIEgen for detection and quantification of  $\text{Hg}^{2+}$  bioaccumulation in algae and  $\text{Hg}^{2+}$  release from algae after bioaccumulation.<sup>21</sup> Such applications can be further explored to detect  $\text{Hg}^{2+}$  dynamics in other organisms in aquatic ecosystems. In this study, we used a specially designed AIEgen to quantitatively evaluate the bioaccumulation of  $\text{Hg}^{2+}$  within a rotifer, and for the first time used this AIEgen to visualize  $\text{Hg}^{2+}$  kinetics *in vivo* within the rotifer in salt water, to better understand the bioaccumulation process using a novel and simple method. This study provides further understanding of the mechanism of interaction between heavy metal ions and small organisms in aquatic systems.

## Materials and methods

### Materials

All reagents were obtained from Sigma-Aldrich (Australia) unless otherwise specified. Stock solutions of AIEgen (*m*-TPE-RNS) and  $\text{HgCl}_2$  at a concentration of 1.0 mM were prepared and stored as previously reported.<sup>21</sup>

The rotifer *Brachionus plicatilis* was obtained from College of Science and Engineering, Flinders University, with a mean length of 80–180  $\mu\text{m}$ . Microalgae *Nannochloropsis oculata* and baker's yeast were used to feed the rotifers at a density  $>400$  ind  $\text{mL}^{-1}$ . Before the test, only yeast was used to minimize the effects of algal pigment on the AIEgen's fluorescence. Stock suspensions of yeast were made by vortexing 3 g dry yeast in 60 ml distilled water, stored at 4 °C, and fed at 0.1 g per million rotifers. *Nannochloropsis oculata* were cultured according to a reported method.<sup>21</sup>

The AIE test solution for staining rotifers contained 10  $\mu\text{M}$  *m*-TPE-RNS. The test solutions for  $\text{Hg}^{2+}$  determination contained 10  $\mu\text{M}$  *m*-TPE-RNS and various  $\text{Hg}^{2+}$  concentrations in the form of  $\text{HgCl}_2$ . The photoluminescence (PL) intensity was read on a fluorescence spectrometer (Varian, Australia) with the excitation wavelength at 355 nm.

### Optimization for staining $\text{Hg}^{2+}$ with AIE in salt water

A salinity ladder (0, 5, 10, 15, 20, 25, 30, and 35 practical salinity unit) was prepared with filtered sea water and distilled water. The salinity was confirmed by a refractometer. After mixing 10  $\mu\text{L}$  of the *m*-TPE-RNS stock solution with 390  $\mu\text{L}$



acetonitrile (ACN) and 590  $\mu\text{L}$  water at different salinities, 10  $\mu\text{L}$  of  $\text{Hg}^{2+}$  stock solution was added. The PL intensity was measured at 1, 5, 15, 30, and 45 min on the fluorescence spectrometer to determine the peak absorption value over time. The effect of salinity on the PL intensity in AIE and  $\text{Hg}^{2+}$  reaction is shown in Fig. S1† and the effect of elapsed time on the PL intensity in AIE and  $\text{Hg}^{2+}$  reaction is shown in Fig. S2.†

To develop a master curve for  $\text{Hg}^{2+}$  determination, a series of  $\text{Hg}^{2+}$  concentrations (1, 5, 10, 20, and 30  $\mu\text{M}$ ) were detected at a constant AIE concentration (10  $\mu\text{M}$ ) over the abovementioned time periods. After the PL intensity was obtained, the PL master curve was developed to show the relationships between PL intensities and  $\text{Hg}^{2+}$  concentrations. The  $\text{Hg}^{2+}$  concentration could be quantified by the corresponding PL intensity measured using the fluorescence spectrometer.

### Quantitative test of $\text{Hg}^{2+}$ bioaccumulation by rotifers

Rotifers were harvested from an aquarium tank with a 50  $\mu\text{m}$  mesh net and rinsed with tap water, and then introduced into a series of water samples containing different  $\text{HgCl}_2$  concentrations (1, 2.5, 5, and 10  $\mu\text{M}$ ) with a rotifer density of 1000 ind  $\text{mL}^{-1}$  for 1 h, followed by a period of recovery in clean water for 24 h. Live and dead rotifers were counted from each treated sample using an optical microscope (Leica, USA) and the survival rate was calculated to determine the toxic response of rotifers to  $\text{Hg}^{2+}$ . The survival rate of rotifers after 1 h of incubation at different concentrations of  $\text{Hg}^{2+}$  is shown in Fig. S3† and the typical optical images of live, dead and live rotifers with eggs are shown in Fig. S4.†

For bioaccumulation of  $\text{Hg}^{2+}$  in rotifers, *B. plicatilis* were harvested and washed using the method above, and were adjusted to a density of 600 ind  $\text{mL}^{-1}$  with clean water, to which  $\text{HgCl}_2$  was added to reach a final concentration of 5  $\mu\text{M}$ . The rate of  $\text{Hg}^{2+}$  absorption by algae was measured at 5, 10, 15, 20, 25, 30, and 45 min. Before each measurement of  $\text{Hg}^{2+}$  concentration in the solution, the rotifers were removed using the mesh net. Briefly, the  $\text{Hg}^{2+}$  concentration in 600  $\mu\text{L}$  of supernatant was determined at 400  $\mu\text{L}$  AIE in the ACN solution to reach a water:ACN ratio of 3:2. AIEgens formed nanoparticles with a mean size of 159 nm, as shown in Fig. S5.† The PL intensity of the stained solution was read on the fluorescence spectrometer.

To determine the  $\text{Hg}^{2+}$  absorption by rotifers, a series of rotifer densities (120, 240, 360, 480, and 500 ind  $\text{mL}^{-1}$ ) were prepared by diluting the stock rotifer culture with clean water.  $\text{HgCl}_2$  was added to each sample to reach a final  $\text{Hg}^{2+}$  concentration of 5  $\mu\text{M}$ . After incubation for 20 min, the rotifers were removed using a mesh net. The  $\text{Hg}^{2+}$  remaining in the solution was determined by the AIE method with an AIE concentration of 5  $\mu\text{M}$ . Then, the amount of  $\text{Hg}^{2+}$  residue in the culture medium was measured by the AIE method using the fluorescence spectrometer and the PL readings were

converted to  $\text{Hg}^{2+}$  concentrations using the developed master curve.

### In vivo visualization of the dynamics of $\text{Hg}^{2+}$ within rotifers by AIEgens

Rotifers were harvested as per the method above, and were adjusted to a density of 1000 ind  $\text{mL}^{-1}$  with clean water and incubated with  $\text{HgCl}_2$  at a concentration of 5  $\mu\text{M}$  for 20 min. They were then transferred into clean water after 20, 60, 180, and 240 min, and stained using the *m*-TPE-RNS working solution at a final concentration of 1  $\mu\text{M}$ . An AIE working solution was prepared by diluting the AIE stock solution in ACN and mixing it with water (v/v, 2:3) to a concentration of 50  $\mu\text{M}$ . After rinsing twice, the rotifers were subjected to imaging using a Leica TCS SP5 scanning confocal microscope. For the fluorescence imaging, the wavelength of blue and red channels was set at 460–500 nm, and 570–610 nm, respectively, but the excitation wavelength was 405 nm.

As a supplement to the fluorescence images, spectral analysis of  $\text{Hg}^{2+}$  was conducted on the rotifers. Our optical characterization system consisted of an in-house scanning fluorescence confocal microscope<sup>22</sup> using a 100 $\times$  objective lens (NA = 0.9) with low background fluorescence for excitation and signal collection, and diffraction-limited spatial resolution ( $\sim 300$  nm). A 532 nm diode laser was used for excitation of the samples with an excitation power of 1 mW. The illuminating position of the laser beam on the samples was controlled by a scanner, and the maximum image area of the samples was 200  $\mu\text{m} \times 200 \mu\text{m}$  with the scan step size down to 300 nm. The fluorescence signal was collected through a 532 nm notch filter and then a long-pass filter with two short cut-off wavelengths (540 nm and 630 nm), and coupled to a multimode fiber for spectral analysis using a commercial spectrometer. Thus, the background fluorescence from the tissue with its high percentage located in the short wavelength range ( $< 630$  nm) was removed. The schematic drawing of the scanning confocal microscope configuration is shown in Fig. S6.†

## Results and discussion

### Physiology of the rotifer and mechanisms of AIE for $\text{Hg}^{2+}$ sensing

In the present study, the rotifer *Brachionus plicatilis* was used to characterize  $\text{Hg}^{2+}$  absorption in small zooplankton that are widely distributed in brackish water; rotifers occasionally numerically dominate zooplankton communities due to their high reproductive rates.<sup>23</sup> The rotifer *B. plicatilis* is an efficient grazer of microalgae and bacteria, linking the primary producers with secondary consumers in an ecosystem, and is one of the most studied rotifer species in ecotoxicology and aquaculture.<sup>19</sup> Like other rotifer species, *B. plicatilis* reproduces by cyclical parthenogenesis, a lifecycle asexual reproduction without males. Typically, the population of female rotifers grows parthenogenetically (asexual reproduction), whereby amictic (asexual) females produce mitotic diploid



eggs. These eggs hatch into genetically identical amictic females. Despite their minute size in the range of 40–200  $\mu\text{m}$ , female rotifers are anatomically complex (Fig. 1).

The detection mechanism of a specific AIEgen for  $\text{Hg}^{2+}$  has been reported.<sup>19</sup> For application in chemical and biological sensing, a highly specific reaction of thiosemicarbazides to form 1,3,4-oxadiazoles triggered by  $\text{Hg}^{2+}$  is adopted for recognition of  $\text{Hg}^{2+}$ . In the absence of  $\text{Hg}^{2+}$ , the sensors are hydrophobic and tend to form aggregates in water. Due to the non-missive spirolactam form of rhodamine, only the blue emission of the tetraphenylethene (TPE) aggregate is expected. After treatment with  $\text{Hg}^{2+}$ , positively charged rhodamine fluorophores are generated, and their solubility in water is greatly increased. In consequence, TPE emission cannot be observed due to the process of dark through-bond energy transfer (DTBET) and non-radiative decay, whereas emission of rhodamine is intensified. Thus, ratiometric  $\text{Hg}^{2+}$  detection could be realized by this rational design strategy (Fig. 2).

### Quantitative evaluation of bioaccumulation of $\text{Hg}^{2+}$ by the rotifer

Numerous studies have shown that Hg is highly toxic. Concentrations at or lower than 0.005  $\text{mg L}^{-1}$  (0.018  $\mu\text{M}$ ) cause reduction in both survival and reproduction of various species of *Brachionus* including *B. rubens*<sup>25</sup> and *B. patulus*.<sup>26</sup> However, the severity of heavy metal toxicity is influenced by various factors such as temperature and food concentration.

Bioaccumulation of  $\text{Hg}^{2+}$  within rotifers can be quantitatively evaluated by the AIEgen method.<sup>21</sup> Several interesting observations were obtained during the evaluation of rotifer bioaccumulation. Rotifers could quickly absorb  $\text{Hg}^{2+}$  and the remaining  $\text{Hg}^{2+}$  ions in the solution after rotifer absorption were quantified using the master curve (Fig. S7†). Fig. 3 shows that a significant drop in  $\text{Hg}^{2+}$  concentration in the medium occurred at the very beginning at a  $\text{Hg}^{2+}$  concentration of 5  $\mu\text{M}$ , indicating the significant initial uptake of  $\text{Hg}^{2+}$  by rotifers. The concentration of  $\text{Hg}^{2+}$  levelled off and plateaued after 5 min. Therefore, 20 min was used as the incubation time in the subsequent study.

Rotifer density is another important parameter influencing the process of bioaccumulation. With an increase in roti-

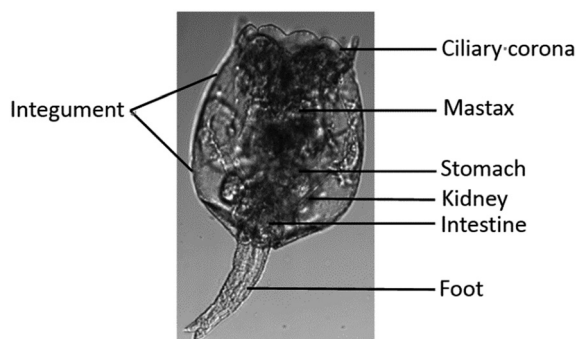


Fig. 1 Structure of the rotifer *Brachionus plicatilis*.<sup>24</sup>

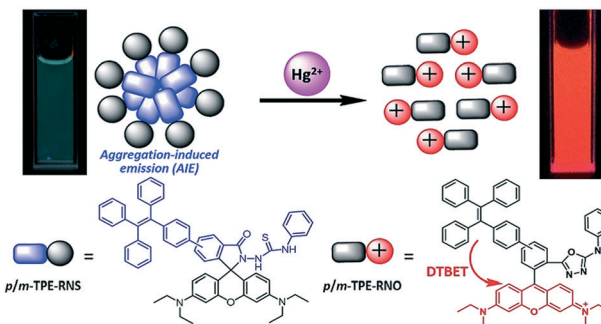


Fig. 2 Schematic illustration of the ratiometric  $\text{Hg}^{2+}$  sensing mechanism of TPE-RNS.<sup>19</sup>

fer density, the amount of  $\text{Hg}^{2+}$  bioaccumulation increased in the rotifer (Fig. S8†). In the solution with 1.355  $\mu\text{g mL}^{-1}$   $\text{HgCl}_2$  (5  $\mu\text{M}$ ), the bioaccumulation efficiency of  $\text{Hg}^{2+}$  decreased from 5.28  $\mu\text{g mg}^{-1} \text{h}^{-1}$  at a rotifer density of 0.093  $\text{mg mL}^{-1}$  to 2.61  $\mu\text{g mg}^{-1} \text{h}^{-1}$  when the rotifer density increased to 0.375  $\text{mg mL}^{-1}$  (Fig. 4).

### In vivo visualization of $\text{Hg}^{2+}$ dynamics within rotifers by AIEgens

The *m*-TPE-RNS based AIEgens have been used for  $\text{Hg}^{2+}$  detection in living cells.<sup>19</sup> The potential  $\text{Hg}^{2+}$  sensing performance of *m*-TPE-RNS in solution motivated us to evaluate its application in  $\text{Hg}^{2+}$  imaging in living rotifers. The rotifers were incubated in a 5  $\mu\text{M}$   $\text{HgCl}_2$  solution for 1 h. After washing with clean water, they were stained with 1  $\mu\text{M}$  *m*-TPE-RNS for 1 h and imaged using confocal laser scanning microscopy. A strong emission in the red channel 570–610 nm was observed along the rotifer digestive tract, especially around the esophagus and mastax (a tooth-like structure for chewing). However, a moderate emission intensity in the blue channel 460–500 nm was detected only in rotifers incubated with the AIEgen, in which the majority of fluorescence was

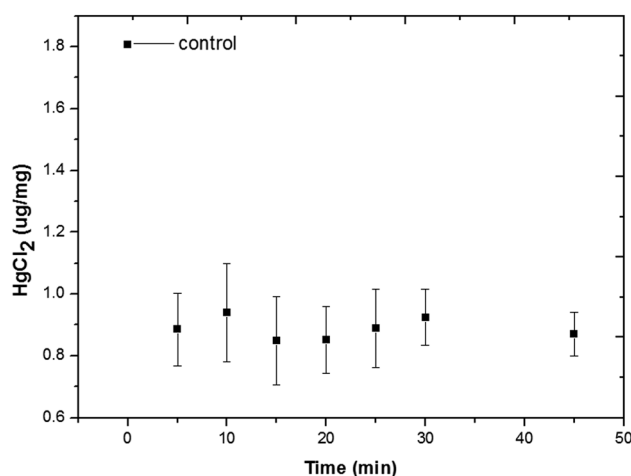


Fig. 3 Amount of bioaccumulation of rotifers at a  $\text{Hg}^{2+}$  concentration of 5  $\mu\text{M}$  over time.



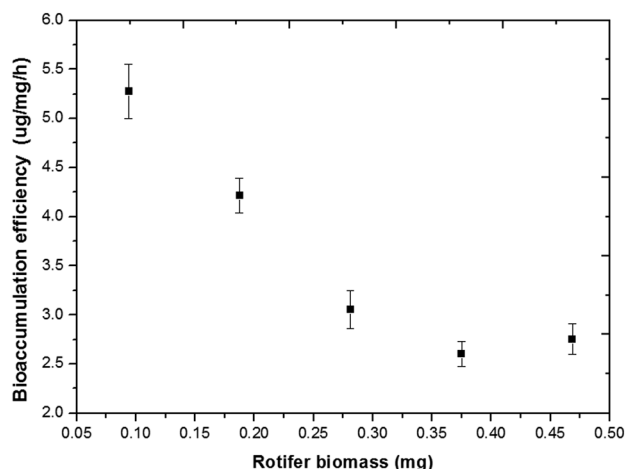


Fig. 4 Bioaccumulation efficiency of  $\text{Hg}^{2+}$  ( $\text{HgCl}_2$ , 5  $\mu\text{M}$ , 1.355  $\mu\text{g mL}^{-1}$ ) at different rotifer densities ( $\text{mg mL}^{-1}$ ) within 20 min.

also excited from the mastax. Rotifers in the absence of  $\text{Hg}^{2+}$  and AIEgen showed weak fluorescence signals in the blue and red channels 570–610 nm. The blue to red color of the merged image indicates a distinct increment of  $\text{Hg}^{2+}$  at the intracellular level after  $\text{Hg}^{2+}$  incubation (Fig. 5). Rotifers incubated with the AIEgen, or  $\text{Hg}^{2+}$  and AIEgen showed fluorescence along the digestive tract, especially around the mastax, suggesting that the AIEgen in the solution could enter the animal body through feeding.

The accumulation of  $\text{Hg}^{2+}$  in phytoplankton occurs by passive diffusion across the cell membrane.<sup>27</sup> In contrast to algae, the manner of  $\text{Hg}^{2+}$  transfer into zooplankton is not

clear. In the present study, the fluorescence results showed that  $\text{Hg}^{2+}$  was visualized around the rotifer body surface (Fig. 6a1 and a2) and within the digestive tract (Fig. 6b). It is reasonable to infer that inorganic  $\text{Hg}^{2+}$  can enter the digestive organ of the rotifer by ingestion, and  $\text{Hg}^{2+}$  cannot permeate into the rotifer by diffusion through the integument. Presumably, this is due to the particular structure of the rotifer integument, which is composed of a thick external layer and a thin internal layer with dense material.<sup>28,29</sup>

Our results demonstrated that the rotifers incubated with  $\text{Hg}^{2+}$  and stained with the AIEgen showed obvious fluorescence along the digestive organ (Fig. 6b). A clearing test was performed to monitor the kinetic transferring of  $\text{Hg}^{2+}$  within the rotifer body. Rotifers could ingest  $\text{Hg}^{2+}$  via their ciliary corona (Fig. 7a). After the rotifers had been transferred into clean water for 20 min,  $\text{Hg}^{2+}$  could be viewed in the mastax (Fig. 7b1 and 8b) and flame cells (functional kidney, Fig. 7b2 and 8b). Our result is supported by a previous study on fish where most of the ingested inorganic and organic  $\text{Hg}^{2+}$  ions were distributed in the muscle, kidney, gonad, liver and gut.<sup>30</sup> However, the distribution of mercury in the body of zooplankton has not been reported. This study was the first to use AIEgen fluorescence as a tool to visualize  $\text{Hg}^{2+}$  distribution in rotifer tissues after  $\text{Hg}^{2+}$  intake.

The fluorescence in the rotifers decreased over time from 40 min after the rotifers were transferred from the  $\text{Hg}^{2+}$  solution into clean water and almost disappeared in 360 min (Fig. 7c–e), indicating that  $\text{Hg}^{2+}$  could dissipate from the rotifer body via the processes of defecation and excretion. A scanning fluorescence confocal microscope with a spectral analysis system was used for the validation of  $\text{Hg}^{2+}$  distribution in the rotifer body, using the AIEgen for *in vivo* visualization for the first time, as shown in Fig. 8. The inserts in Fig. 8(c) and (d) (detailed information shown in ESI† Fig. S10) show the PL spectra of two selected points in the fluorescence images of Fig. 8(c) and (d), respectively. The spectrum of the point with red color in Fig. 8(d) shows more than 10 times higher PL intensity at a wavelength of 590 nm than that of the spectrum of the point with blue color in Fig. 8(c), which indicates that the red color in the fluorescence image in Fig. 8 represents the accumulation areas of  $\text{Hg}^{2+}$  in the rotifer.

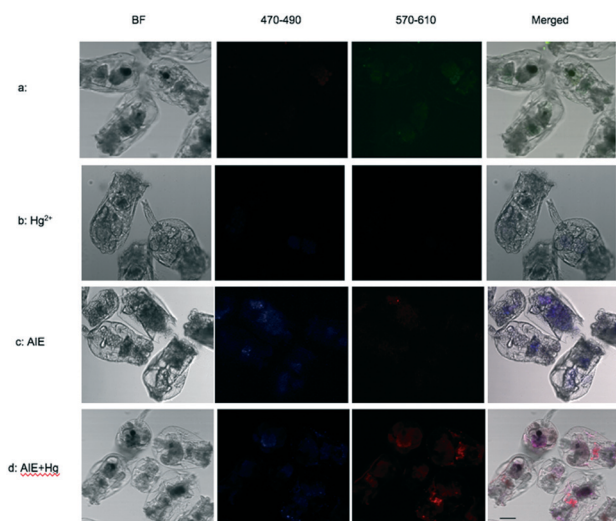


Fig. 5 Confocal microscopy images of  $\text{Hg}^{2+}$  in rotifers using AIEgens. (a) The control without  $\text{Hg}^{2+}$  in rotifers and AIEgen staining; (b) rotifers exposed to  $\text{Hg}^{2+}$ , without the presence of AIEgens, show only weak fluorescence in the gut, either in the red channel 570–610 nm or the blue channel 460–500 nm; (c) rotifers exposed to AIEgens without  $\text{Hg}^{2+}$  show fluorescence in the gut, but are brighter in the blue channel than in the red channel; (d) rotifers exposed to  $\text{Hg}^{2+}$  stained with AIEgens show brighter fluorescence in the gut in the red channel than in the blue channel. Bar = 50  $\mu\text{m}$ .

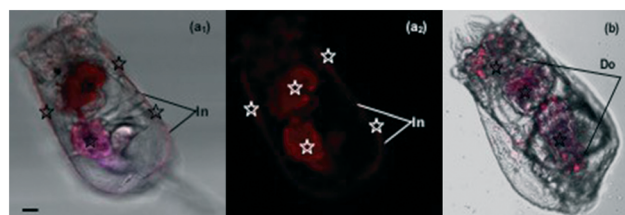
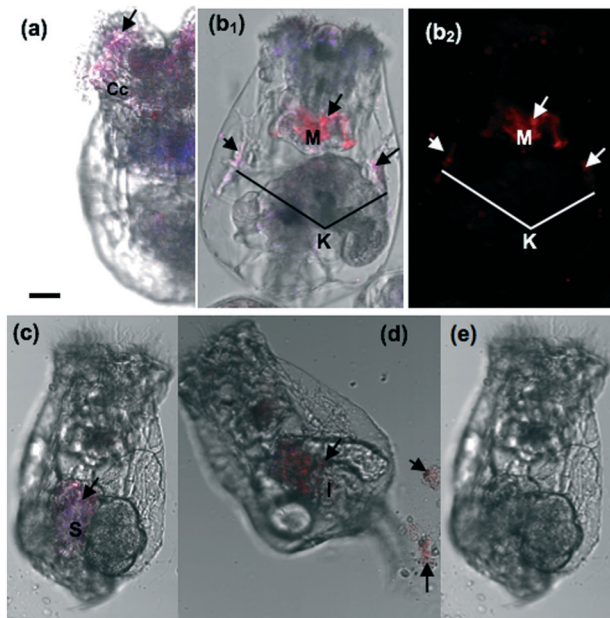
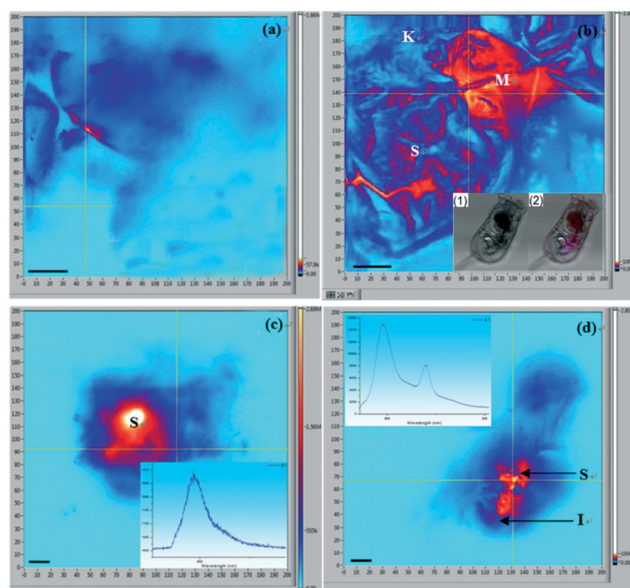


Fig. 6 Fluorescence images of  $\text{Hg}^{2+}$  moving into the rotifer as shown by the AIEgen. (a1: white background) & (a2: black background):  $\text{Hg}^{2+}$  is blocked outside by the lorica. (b):  $\text{Hg}^{2+}$  visualized within the digestive system of the rotifer.  $\text{Hg}^{2+}$  (☆) is located where red fluorescence is visualized. In: integument; Do: digestive organ. Bar = 15  $\mu\text{m}$ .





**Fig. 7** Fluorescence images of the  $\text{Hg}^{2+}$  clearing test within a rotifer visualized *in vivo* using the AIEgen. (a)  $\text{Hg}^{2+}$  is ingested by the ciliary corona of a rotifer; (b) rotifers incubated with  $\text{Hg}^{2+}$  for 20 min and then transferred into clear water and stained with *m*-TPE-RNS at 20 min, (c) 60 min, (d) 180 min (e) and 240 min with an excitation wavelength of 350 nm. Cc: ciliary corona; M: mastax; K: kidney; S: stomach; I: intestine. Arrows:  $\text{Hg}^{2+}$ ; bar = 15  $\mu\text{m}$ .



**Fig. 8** Spectral analysis images of a rotifer (a) without  $\text{Hg}^{2+}$  and with 5  $\mu\text{M}$   $\text{Hg}^{2+}$  for (b) 45 min, (c) 45 min, and (d) 90 min; inserts in (b) show a rotifer image under (1) a normal optical microscope and (2) a confocal optical microscope; inserts in (c) and (d) show the spectra of the blue and red images inside a rotifer, respectively. K: kidney; M: mastax; S: stomach; I: intestine. Bar = 15  $\mu\text{m}$ .

Interestingly,  $\text{Hg}^{2+}$  could no longer be observed within the kidneys during this period (Fig. 7c–e, 8c and d). Firstly, the  $\text{Hg}^{2+}$  was distributed in the stomach and intestine, but not in

the flame cells (kidneys) after 40 min. This phenomenon is similar to a report on fish where the intestinal wall is an effective barrier to  $\text{HgCl}_2$  but is permeable to  $\text{MeHg}$ .<sup>31</sup> Secondly, besides defecation through the digestive tract,  $\text{Hg}^{2+}$  could be excreted through the kidney, as fluorescence ( $\text{Hg}^{2+}$ ) totally disappeared from within the rotifers after 360 min (Fig. 7e). Consequently, we can infer that inorganic mercury is not easily retained in rotifer tissues, though it can quickly enter rotifers *via* feeding (Fig. 3).

Previous studies have confirmed that in comparison with  $\text{Hg}^{2+}$ ,  $\text{MeHg}$  is more toxic and more readily accumulated by aquatic biota because of its lipophilic and protein-binding properties.<sup>32,33</sup> Methylation of mercury in the aquatic environment is a critical step towards the accumulation of mercury in the aquatic food chain, and  $\text{MeHg}$  is produced in the environment primarily by anaerobic bacteria<sup>34</sup> or by some specific macroalgae.<sup>35</sup> According to our fluorescence results, it seems that mercury methylation is unlikely in rotifers, which is one trophic link above algae. Further research is warranted to determine if the direct intake of  $\text{MeHg}$  would lead to mercury deposition in rotifers.

## Conclusions

In this study, we used a specially designed AIEgen to quantitatively evaluate the bioaccumulation of  $\text{Hg}^{2+}$  in rotifers, which is the first time that an AIEgen is used to visualize  $\text{Hg}^{2+}$  kinetics *in vivo* within rotifers in salt water to better understand the bioaccumulation process using a simple procedure. Our quantitative results showed that a significant drop in PL intensity occurred at the very beginning after  $\text{Hg}^{2+}$  addition, indicating a fast initial uptake of  $\text{Hg}^{2+}$  by the rotifers. The amount of bioaccumulation increased with the rotifer density, but the bioaccumulation efficiency of  $\text{Hg}^{2+}$  decreased with the rotifer quantity. The distribution of  $\text{Hg}^{2+}$  was visualized within the digestive tract, excretory organ and body surface of the rotifers using fluorescence images and spectrum analyses. It seems that inorganic  $\text{Hg}^{2+}$  is accumulated in the rotifer digestive organ *via* food ingestion, and  $\text{Hg}^{2+}$  could not diffuse into the rotifer *via* the body integument. Although inorganic mercury can enter rotifers through food ingestion, it is unlikely that  $\text{Hg}^{2+}$  can be methylated and deposited in rotifers. Future study should further investigate the difference between bioaccumulation of inorganic and organic mercury.

## Conflicts of interest

There are no conflicts to declare.

## Acknowledgements

Y. Jiang and T. He are grateful for the support of the China Scholarship Council with visiting scholar programs to Flinders University. Y. Tang is grateful for the support of Flinders University through a Faculty of Science and Engineering Establishment Grant.



## Notes and references

- 1 M. F. Gutierrez, A. M. Gagneten and J. C. Paggi, *Ecotoxicology*, 2012, 21(1), 37–47.
- 2 R. A. Lavoie, T. D. Jardine, M. M. Chumchal, K. A. Kidd and L. M. Campbell, *Environ. Sci. Technol.*, 2013, 47(23), 13385–13394.
- 3 O. Dalman, A. Demirak and A. Balci, *Food Chem.*, 2006, 95(1), 157–162.
- 4 U. Daewel, S. S. Hjollo, M. Huret, R. Ji, M. Maar, S. Niiranen, M. Travers-Trolet, M. A. Peck and K. E. van de Wolfshaar, *ICES J. Mar. Sci.*, 2014, 71(2), 254–271.
- 5 J. S. Gray, *Mar. Pollut. Bull.*, 2002, 45(1–12), 46–52.
- 6 K. A. Kidd, D. C. G. Muir, M. S. Evans, X. Wang, M. Whittle, H. K. Swanson, T. Johnston and S. Guidford, *Sci. Total Environ.*, 2012, 438, 135–143.
- 7 L. M. Campbell, R. J. Norstrom, K. A. Hobson, D. C. G. Muir, S. Backus and A. T. Fisk, *Sci. Total Environ.*, 2005, 351, 247–263.
- 8 C. J. Watras, R. C. Back, S. Halvorsen, R. J. M. Hudson, K. A. Morrison and S. P. Wente, *Sci. Total Environ.*, 1998, 219(2–3), 183–208.
- 9 F. A. P. C. Gobas, W. de Wolf, L. P. Burkhard, E. Verbruggen and K. Plotzke, *Integr. Environ. Assess. Manage.*, 2009, 5, 624–637.
- 10 B. C. Kelly, M. G. Ikonomou, J. D. Blair, A. E. Morin and F. A. P. C. Gobas, *Science*, 2007, 317, 236–239.
- 11 C. J. Watras, R. C. Back, S. Halvorsen, R. J. M. Hudson, K. A. Morrison and S. P. Wente, *Sci. Total Environ.*, 1998, 219, 183–208.
- 12 M. T. K. Tsui and W.-X. Wang, *Environ. Sci. Technol.*, 2004, 38(3), 808–816.
- 13 J. Mei, N. L. C. Leung, R. T. K. Kwok, J. W. Y. Lam and B. Z. Tang, *Chem. Rev.*, 2015, 115(21), 11718–11940.
- 14 J. Mei, Y. Hong, J. W. Y. Lam, A. Qin, Y. Tang and B. Z. Tang, *Adv. Mater.*, 2014, 26(31), 5429–5479.
- 15 D. Ding, K. Li, B. Liu and B. Z. Tang, *Acc. Chem. Res.*, 2013, 46(11), 2441–2453.
- 16 F. Guo, W. P. Gai, Y. Hong, B. Z. Tang, J. Qin and Y. Tang, *Chem. Commun.*, 2015, 51(97), 17257–17260.
- 17 S. Chen, H. Wang, Y. Hong and B. Z. Tang, *Mater. Horiz.*, 2016, 3, 283–293.
- 18 Y. Hong, *Methods Appl. Fluoresc.*, 2016, 4, 022003, DOI: 10.1088/2050-6120/4/2/022003.
- 19 Y. Chen, W. Zhang, Y. Cai, R. T. K. Kwok, Y. Hu, J. W. Y. Lam, X. Gu, Z. He, Z. Zhao, X. Zheng, B. Chen, C. Gui and B. Z. Tang, *Chem. Sci.*, 2017, 8(3), 2047–2055.
- 20 Z. Ruan, C. Li, J. Li, J. Qin and Z. Li, *Sci. Rep.*, 2015, 5, 15987, DOI: 10.1038/srep15987.
- 21 Y. Jiang, Y. Chen, M. Alrashdi, W. Luo, B. Z. Tang, J. Qin and Y. Tang, *RSC Adv.*, 2016, 6(102), 100318–100325.
- 22 D. M. Shotton, *J. Cell Sci.*, 1989, 94, 175–206.
- 23 K. Venetia, C. M. Joséand and D. Pascal, *J. Biol. Res.*, 2012, 17, 97–112.
- 24 W. Zhao, L. Q. Wang, G. X. Wang, X. Q. Wang, Q. Liu, Z. J. Li, S. L. Zhang and Y. Han, *Hydrobiology*, China Agriculture Press, China, 2005.
- 25 S. S. S. Sarma, P. S. L. Jurado and S. Nandini, *Rev. Biol. Trop.*, 2001, 49(1), 77–84.
- 26 S. S. S. Sarma, H. F. Nunez-Cruz and S. Nandini, *Dongwu Xuebao*, 2005, 51(1), 46–52.
- 27 J. Gutknecht, *J. Membr. Biol.*, 1981, 61, 61–66.
- 28 K. Bender and W. Kleinow, *Comp. Biochem. Physiol., Part B: Biochem. Mol. Biol.*, 1988, 89(3), 483–487.
- 29 J. Yu and S. Cui, *Hydrobiologia*, 1997, 358, 95–103.
- 30 D. Kasper, E. F. A. Palermo, A. C. M. I. Dias, G. L. Ferreira, R. P. Leitao, C. W. C. Branco and O. Malm, *Neotrop. Ichthyol.*, 2009, 7(4), 751–758.
- 31 World Health Organization (WHO), *Mercury-environmental aspects*, WHO, Switzerland, 1989.
- 32 D. W. Boening, *Chemosphere*, 2000, 40(12), 1335–1351.
- 33 S. M. Ullrich, T. W. Tanton and S. A. Abdrashitova, *Crit. Rev. Environ. Sci. Technol.*, 2001, 31(3), 241–293.
- 34 H. Hsu-Kim, K. H. Kucharzyk, T. Zhang and M. A. Deshusses, *Environ. Sci. Technol.*, 2013, 47(6), 2441–2456.
- 35 R. Pongratz and K. G. Heumann, *Chemosphere*, 1998, 36(9), 1935–1946.

